

Beauty Production at HERA using decays to J/Ψ in the ZEUS detector

Summer Student Program 2010, DESY

Timo Nachstedt
University Göttingen
Supervisor: Olaf Behnke

September 2010

Abstract

This report presents the results of my work during the participation in the DESY summer student program. The aim of my project was to establish a measurement of B hadron production at HERA II using decays to J/Ψ . Therefore I firstly did an inclusive study in which J/Ψ s originating from a secondary vertex were identified by the secondary vertex significance. In a second study I tried to do a complete B reconstruction in the channel $B^\pm \rightarrow J/\Psi K^\pm$.

Contents

1	Physics Motivation	5
2	Inclusive $B \rightarrow J\Psi X$ study	5
2.1	Signal and Background Processes	6
2.2	Dataset used	6
2.3	Secondary Vertex Fit and Significance	7
2.4	Object and Event Selection	7
2.5	J/Ψ Mass and Significance distributions	8
2.6	Signal Fitting in Significance Bins	9
3	$B^\pm \rightarrow J/\Psi K^\pm$ Study	17
3.1	Additional Cuts	17
3.2	Reconstructed B Mass	17
4	Conclusion	21
5	Acknowledgements	21

1 Physics Motivation

The production of B -mesons in electron-proton-collisions as shown in figure 1 provides a good test on perturbative QCD. Furthermore the investigation of B production is directly sensitive to the gluon density in the proton. Until now B production at HERA and HERA II has only been measured in semileptonic decays and with the help of jet inclusive secondary vertexing.

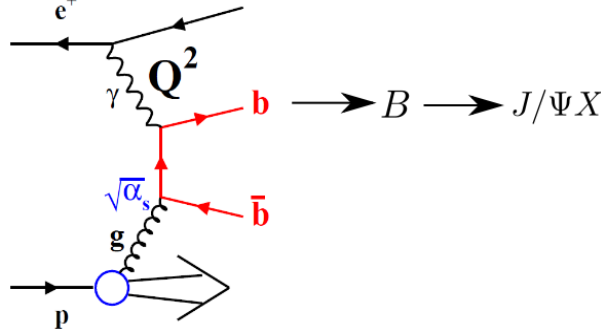


Figure 1: Feynman graph for production of b quarks in positron-proton-collisions.

The approach presented in this report is the investigation of the decay channel $B \rightarrow J/\Psi X$ where the J/Ψ decays into two muons: $J/\Psi \rightarrow \mu^+ \mu^-$. It is an advantage of this channel that one can expect a clean J/Ψ -mass peak which can be used to identify the decay. Furthermore it should in principle be possible to fully reconstruct the B meson for example in the decay $B^\pm \rightarrow J/\Psi K^\pm$. A complete and significant reconstruction of the B meson has never been achieved in HERA or HERA II. Stefan Lueders [1] tried this for HERA, but could only achieve a 2σ -peak.

There are also disadvantages connected with the chosen decay channel. Firstly the reconstruction is very dependent on a high muon reconstruction efficiency. Secondly the branching ratio of the decay channel is quite low. The branching ratio for the inclusive decay to a J/Ψ is approximately one per cent: $BR(B \rightarrow J/\Psi X) \approx 1.1 \cdot 10^{-2}$. The decay to a J/Ψ accompanied by a charged kaon occurs approximately in one out of thousand B^\pm decays: $BR(B^\pm \rightarrow J/\Psi K^\pm) \approx 1.0 \cdot 10^{-3}$. Finally both ratios have still to be multiplied by the fraction of all J/Ψ s that decay into two muons: $BR(J/\Psi \rightarrow \mu\mu) \approx 5.9 \cdot 10^{-2}$.

2 Inclusive $B \rightarrow J\Psi X$ study

In the first study presented in this report I do an inclusive search for J/Ψ particles originating from B mesons. Those J/Ψ s can be distinguished from prompt J/Ψ s because of the fact that the B -meson has a lifetime of $\tau \approx 1.6 \cdot 10^{-12}$ s. This means a B -meson produced at the primary vertex travels a distance in the order of magnitude of $c\tau \approx 490 \mu\text{m}$ before it decays. Its decay products, e.g. the J/Ψ , are therefore produced at a secondary vertex. Those secondary vertices can be reconstructed

with the help of the ZEUS Microvertex Detector (MVD) and the Central Tracking Detector (CTD).

2.1 Signal and Background Processes

The signal process is illustrated in figure 1. The main background for this processes is given by prompt J/Ψ s originating from diffractive and inelastic J/Ψ production. The Feynman graphs for those processes are shown in figures 2 and 3.

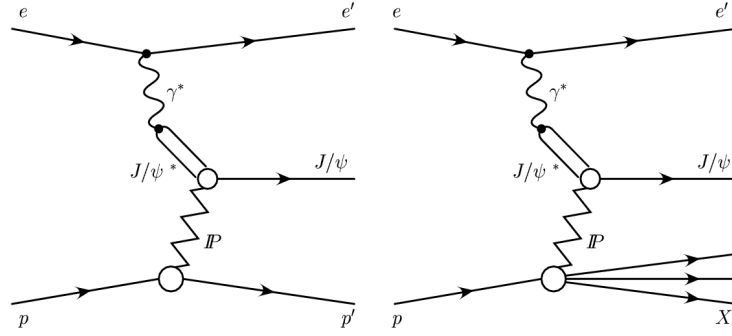


Figure 2: Diffractive J/Ψ production.

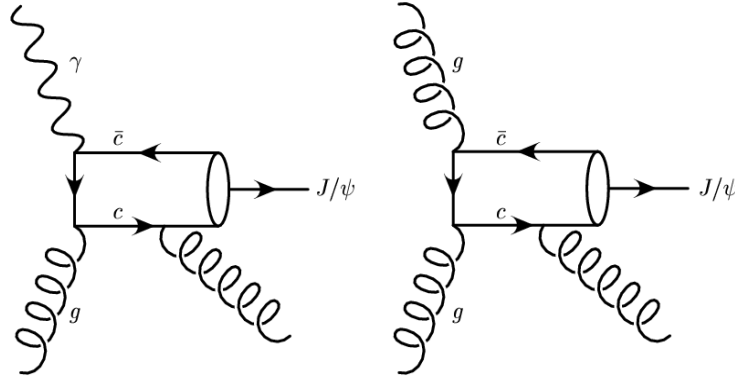


Figure 3: Inelastic J/Ψ production.

2.2 Dataset used

The analyses presented are done using the positron-proton collision data from the years 2004, 2006 and 2007 and the electron-proton collision data from the years 2005 and 2006. The Rapgap inclusive beauty DIS sample is used as Monte Carlo signal sample, the diffractive J/Ψ Monte Carlo Sample is used to understand the background. While the data and Rapgap sample are available in the ZEUS Common NTuple version v04b, the diffractive J/Ψ sample is only available in the NTuple version v02e.

2.3 Secondary Vertex Fit and Significance

To determine if a couple of tracks in the detector have been created by particles originating from a common vertex as well as the position of this vertex a three dimensional vertex fit is performed. This can be done with the help of the *VxLite Vertex Fitter*, which is a part of the *tLite* library created by Hartmut Stadie [2]. To use *vxLite* in combination with the ZEUS Common NTuple the version v04b of the latter is needed. Only this version contains the necessary track helix parameters. For this reason the fit could not be performed for the diffractive J/Ψ sample. Instead of this the already contained informations of the secondary vertex block had to be used. Unfortunately these informations are only present if a jet was found in the event.

The position of the primary vertex is directly read out of the NTuple. Out of primary vertex and secondary vertex the decay length L_{xy} in the transverse plane and its uncertainty $\sigma(L_{xy})$ can be calculated. The significance of the secondary vertex is defined by $S := L_{xy}/\sigma(L_{xy})$

2.4 Object and Event Selection

Only muons out of the GMuon block which fulfill certain criteria are considered for this study. Those criteria are listed below:

- $P_T(\mu) > 0.5 \text{ GeV}$
- $|\eta(\mu)| < 1.5$
- Muon is associated to a ZTT track with
 - $N_{\text{hits}}(\text{MVD}_{\text{Barrel,R}}) > 1$
 - $N_{\text{hits}}(\text{MVD}_{\text{Barrel,Z}}) > 1$
 - CTD Inner Superlayer = 0
 - CTD Outer Superlayer > 2

A J/Ψ -candidate is reconstructed out of the two muons with the highest P_T , where one muon must have a global quality of at least 4 and the other one a quality of at least 0. The tracks of the two muons are used to do a secondary vertex fit.

Further cuts are applied to the global properties of an event. Those are in detail:

- Global Time < 7
- Primary Vertex is fitted
- $|z_{\text{prim. vertex}}| < 30 \text{ cm}$
- $N_{\text{tracks}}(\text{prim. vertex}) > 4$
- $E_{T,\text{Cal}} - E_{T,\text{Cal},10} > 6 \text{ GeV}$

- $y_{JB} > 0.1$

Finally, there a couple of cuts concerning the reconstructed J/Ψ -candidate:

- $q(\mu_1) \cdot q(\mu_2) = -1$
- $\chi^2_{SV}/Ndf < 3$ (χ^2_{SV} : χ^2 of secondary vertex fit)
- $\theta(\mu_1) + \theta(\mu_2) - \pi > 0.1$
- $|\eta(J/\Psi)| < 1.5$
- $P_T(J/\Psi) > 1 \text{ GeV}$
- $z(J/\Psi) = \frac{(E-p_z)_{J/\Psi}}{(E-p_z)_{\text{event}}} < 0.5$

As this study has just an explorative character there is no explicit trigger selection done.

2.5 J/Ψ Mass and Significance distributions

Figure 4 shows the distributions of the reconstructed J/Ψ mass and the significance of the secondary vertex after muon selection and the cuts on global event variables. All J/Ψ candidates that fulfill those cuts are shown, there is no additional mass cut applied. Therefore the distributions are dominated by background processes. Figure 5 shows the same distributions after the cuts on the variables that depend on the reconstructed J/Ψ -candidate.

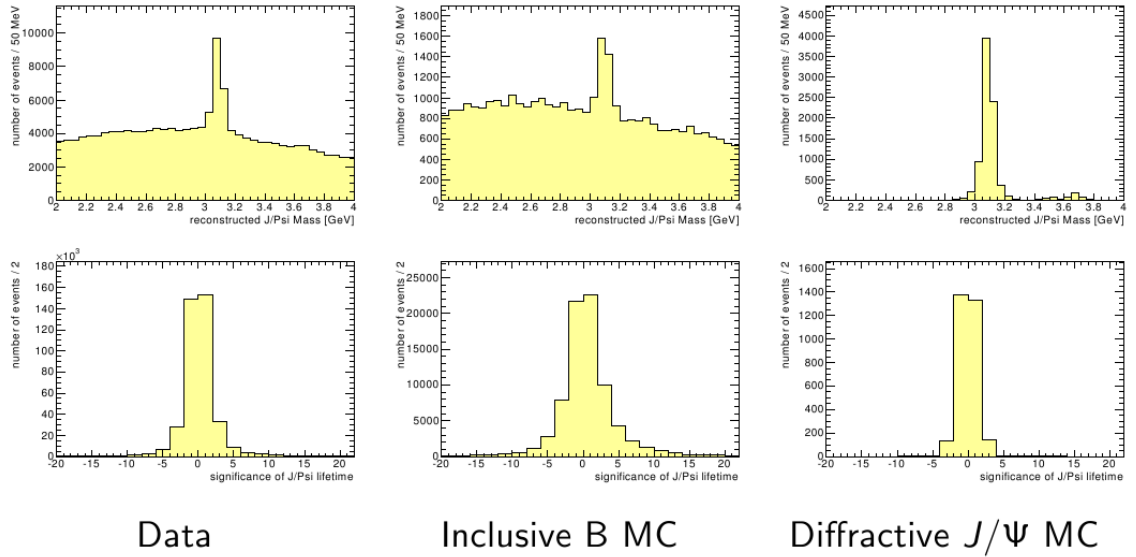


Figure 4: Mass (upper histograms) and secondary vertex significance (lower histograms) distributions in the different samples after the global event cuts.

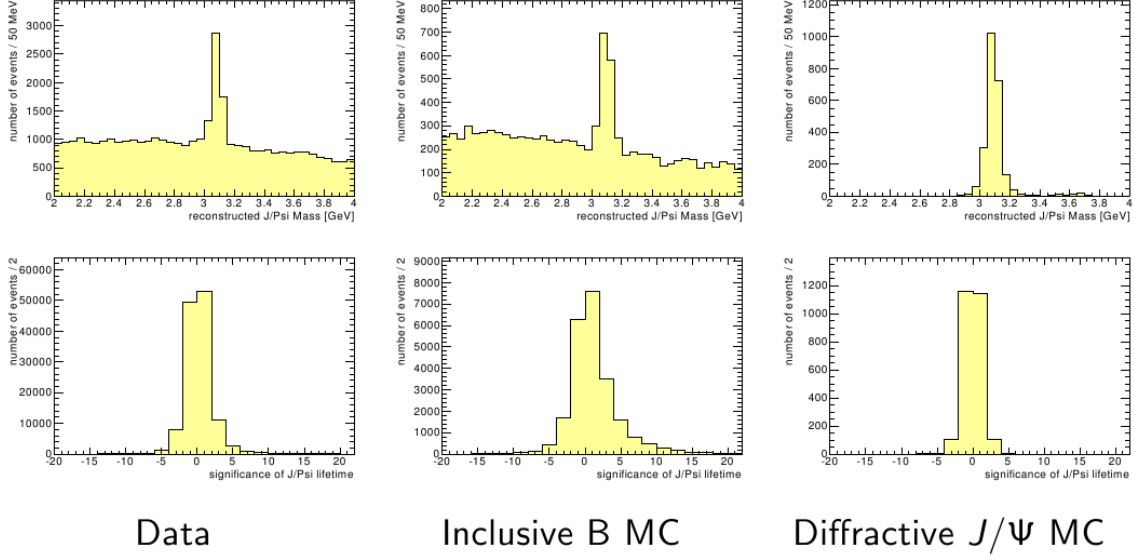


Figure 5: Mass (upper histograms) and secondary vertex significance (lower histograms) distributions in the different samples after the final J/Ψ selection.

2.6 Signal Fitting in Significance Bins

To determine the number of reconstructed J/Ψ s with a certain secondary vertex significance the distribution of the reconstructed mass is studied in different significance bins. In every bin a sum of a second order background polynomial and a normalised Gaussian signal distribution is fitted on the distribution. In doing so the central value of the Gaussian distribution is fixed to the PDG value $m(J/\Psi) \approx 3.097$ GeV and its width is determined by a fit over all J/Ψ -candidates and afterwards also fixed for the fits in the different significance bins. An example fit is shown in fig. 6.

If there are less than hundred events in one histogram, a linear background function is used instead of the polynomial. In case there are less than fifty events in the whole histogram, just a constant fit is used to determine the background. Furthermore the fits are done using the *Loglikelihood* method and the *Minos* technique to estimate the parameter errors.

In a first step there are just two significance bins considered. The first one contains all J/Ψ -candidates with a secondary vertex significance $S < -2$, for the second one it is $S > 2$. The difference of the number of signal events in both bins defines the asymmetry A :

$$A = \text{Signal}(S > 2) - \text{Signal}(S < -2).$$

The uncertainty $\sigma(A)$ is calculated by normal error propagation. The quotient $A/\sigma(A)$ gives the significance level at which J/Ψ s from secondary vertices can be established.

In table 1 the number of fitted signal events and the calculated asymmetry after

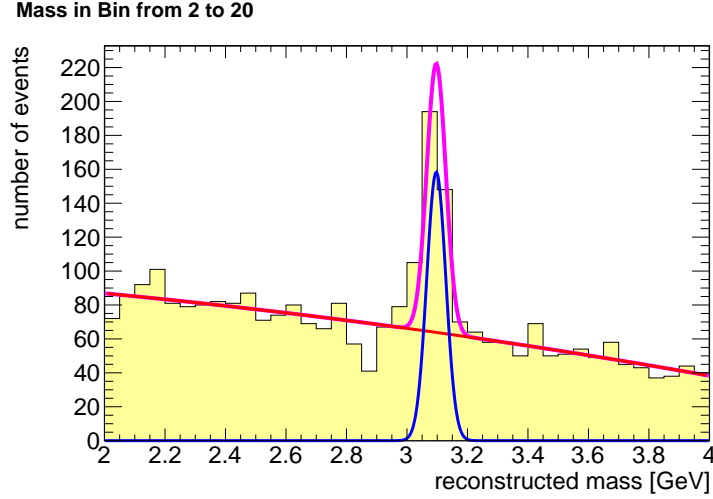


Figure 6: J/ψ mass distribution for $S>2$ in data sample after final J/ψ selection. Red: fitted background, blue: fitted signal, red: total fit.

every cut level is shown for the inclusive B Monte Carlo. A maximum asymmetry significance of 19.1 is achieved. Table 2 lists the same for the data samples. Here a maximum asymmetry significance of 5.0 is found.

In a second step significance bins with a width of 2 are chosen in the range from -20 to 20 . Figure 7 shows the fits in the eight most central bins for the inclusive B Monte Carlo sample. Figure 8 shows the obtained fits for the diffractive J/ψ Monte Carlo sample. Finally the results obtained for data are shown in figure 9.

The fitted number of J/ψ candidates is depicted versus the central value of the significance bin in figure 10 for the B Monte Carlo, in figure 11 for the diffractive J/ψ Monte Carlo and in figure 12 for the data. As expected a huge asymmetry can be observed for the B Monte Carlo while there is no significant asymmetry visible in the diffractive J/ψ Monte Carlo. A zoomed view on the graph for the data sample reveals a clear asymmetry in the bins with a significance $S > 4$ for the data sample as well.

In a further study the shapes of the graphs in the Monte Carlo samples could be used to do a fit on the distribution in the data sample. A rough estimation based on the asymmetries in tables 1 and 2 results in the assumption that there is approximately three to four times as much statistics in the B Monte Carlo as in the Data Monte Carlo. This seems to be in agreement with the graphs 10, 11 and 12.

Cut	$S < -2$	$S > 2$	Asymmetry	Significance
-	43(23)	656(36)	613(42)	14.7
global time < 7	44(23)	655(35)	611(42)	14.7
PV fitted	44(23)	655(35)	611(42)	14.7
$z(\text{PV}) < 30\text{cm}$	44(23)	653(35)	609(42)	14.6
$N_{\text{tracks}}(\text{PV}) > 4$	43(23)	654(35)	611(42)	14.7
$E_{T,\text{Cal}} - E_{T,\text{Cal},10} > 6 \text{ GeV}$	42(23)	655(35)	612(42)	14.8
$y_{\text{JB}} > 0.1$	42(23)	655(35)	612(42)	14.8
$q(\mu_1) \cdot q(\mu_2) = -1$	21(17)	624(31)	603(35)	17.2
$\chi^2/Ndf(SV) < 3$	1(18)	547(28)	545(33)	16.6
$\theta_1 + \theta_2 - \pi > 0.1$	1(18)	547(28)	545(33)	16.6
$ \eta(J/\Psi) < 1.5$	0(5)	496(26)	496(27)	19.0
$P_T(J/\Psi) > 1 \text{ GeV}$	0(3)	493(26)	493(26)	19.1
$z(J/\Psi) < 0.5$	0(3)	493(26)	493(26)	19.1

Table 1: Asymmetry cutflow in the inclusive B Monte Carlo sample.

Cut	$S < -2$	$S > 2$	Asymmetry	Significance
-	3035(69)	3216(70)	181(99)	1.8
global time < 7	3029(69)	3216(70)	187(98)	1.9
PV fitted	3029(69)	3216(70)	187(98)	1.9
$z(\text{PV}) < 30\text{cm}$	3018(69)	3209(70)	190(98)	1.9
$N_{\text{tracks}}(\text{PV}) > 4$	777(46)	1059(48)	281(66)	4.3
$E_{T,\text{Cal}} - E_{T,\text{Cal},10} > 6 \text{ GeV}$	544(42)	817(45)	273(61)	4.5
$y_{\text{JB}} > 0.1$	458(41)	721(44)	263(60)	4.4
$q(\mu_1) \cdot q(\mu_2) = -1$	480(35)	706(38)	226(51)	4.5
$\chi^2/Ndf(SV) < 3$	328(26)	517(30)	189(40)	4.8
$\theta_1 + \theta_2 - \pi > 0.1$	328(26)	517(30)	189(40)	4.8
$ \eta(J/\Psi) < 1.5$	208(20)	358(24)	150(31)	5.0
$P_T(J/\Psi) > 1 \text{ GeV}$	235(22)	398(26)	163(33)	4.9
$z(J/\Psi) < 0.5$	127(18)	250(22)	122(28)	4.4

Table 2: Asymmetry Cutflow in the Data sample.

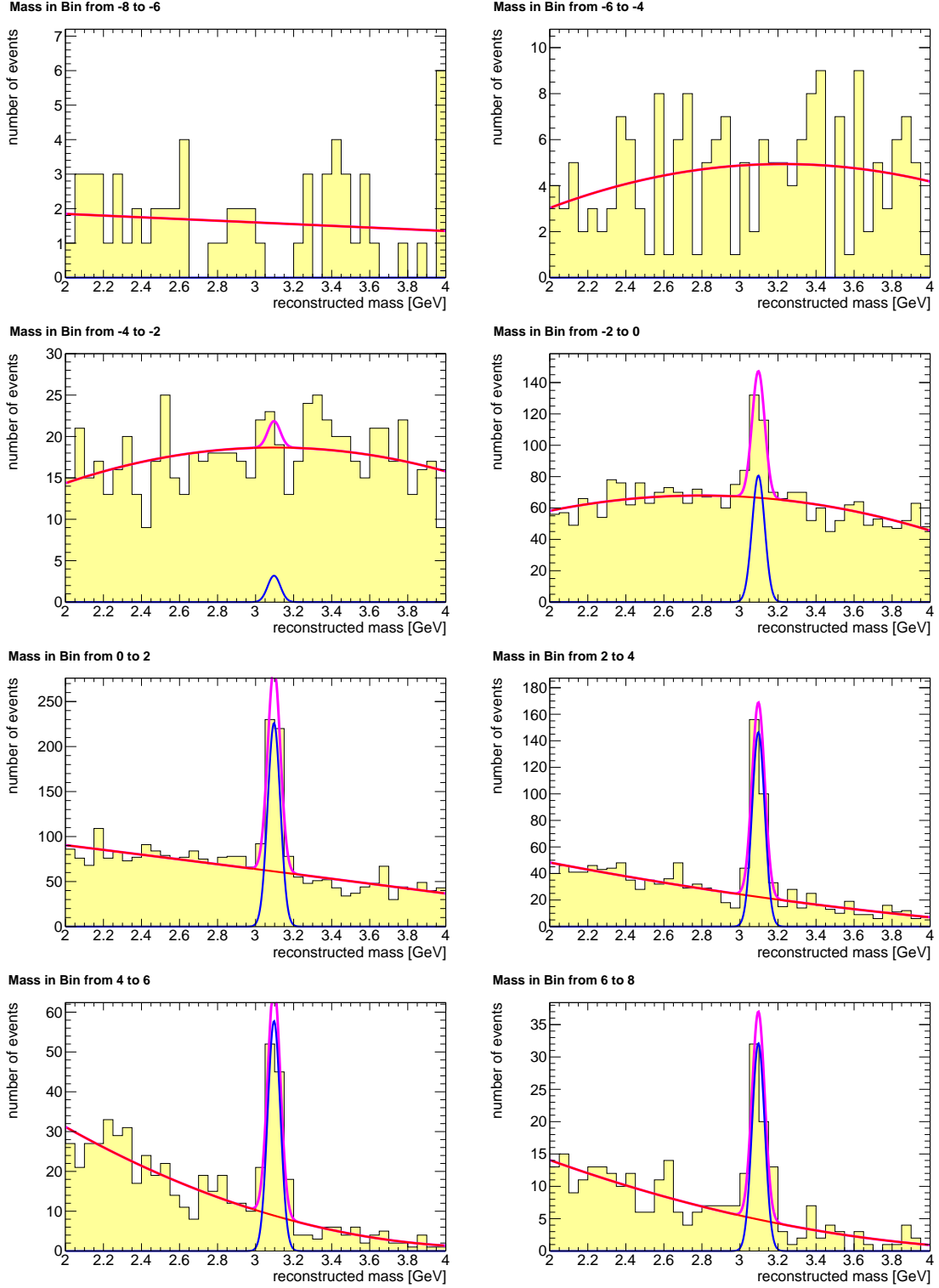


Figure 7: Fitted mass distribution in significance bins for the inclusive B Monte Carlo.

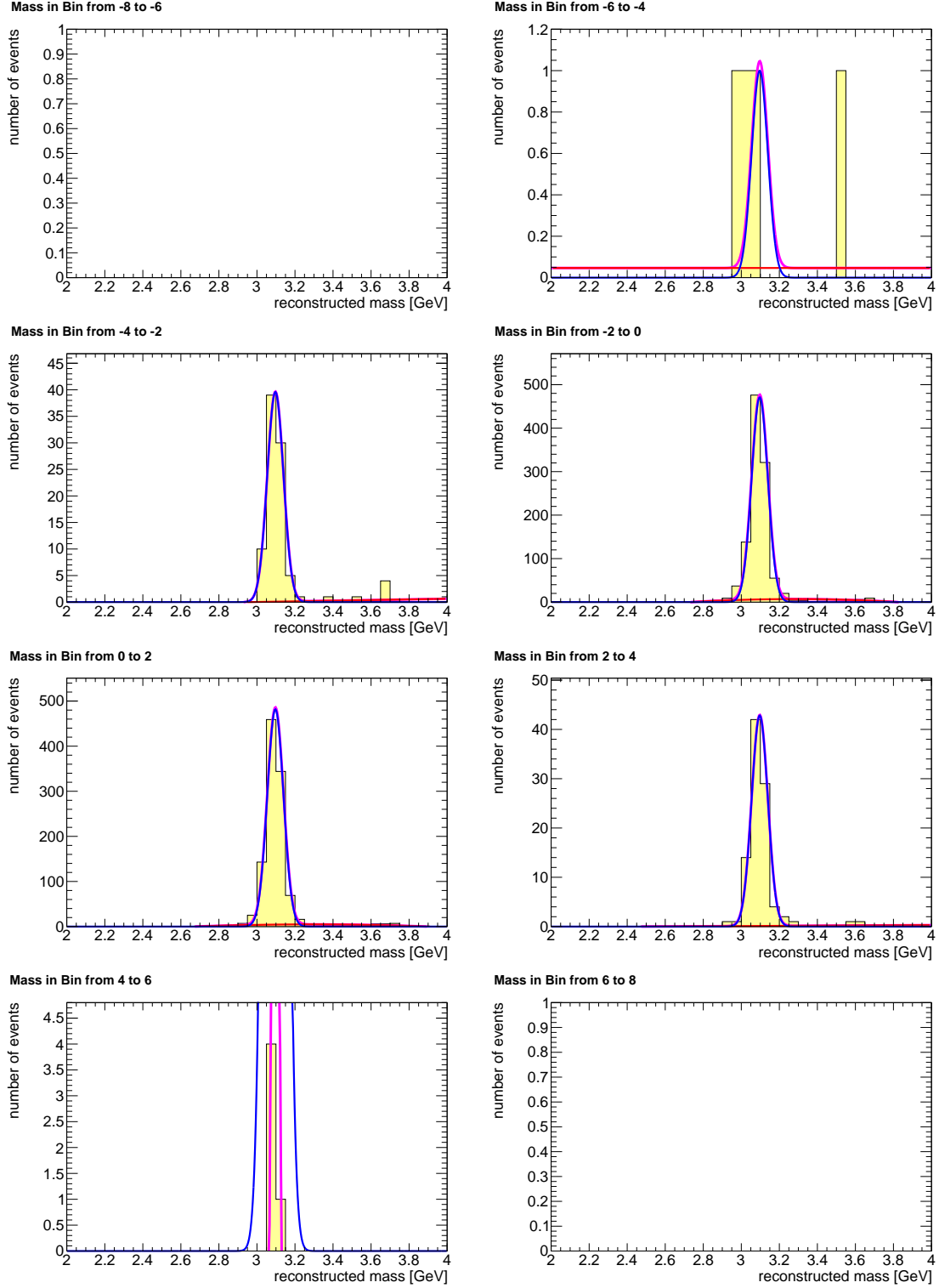


Figure 8: Fitted mass distribution in significance bins for the diffractive J/Ψ Monte Carlo.

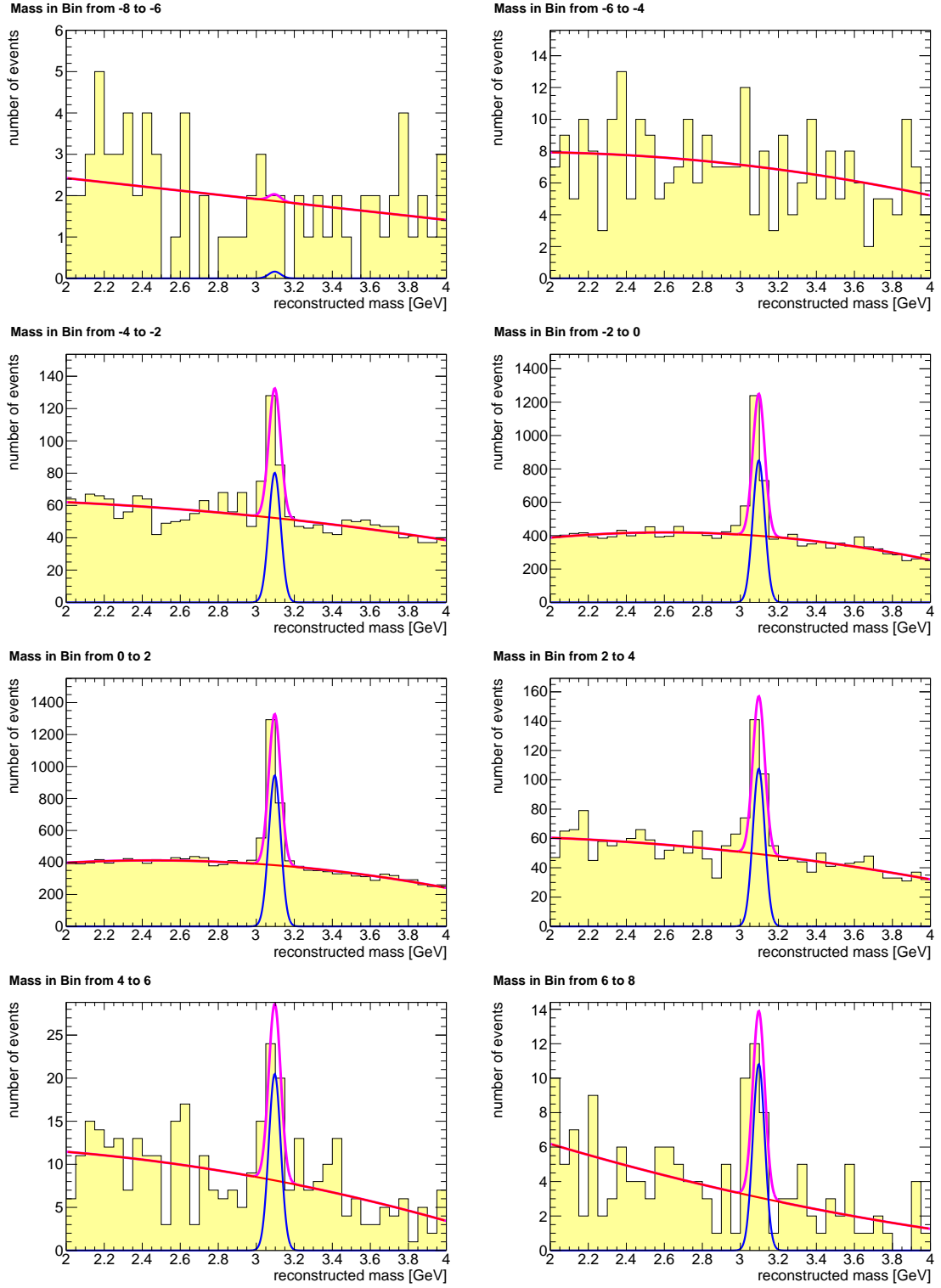


Figure 9: Fitted mass distribution in significance bins for the data sample.

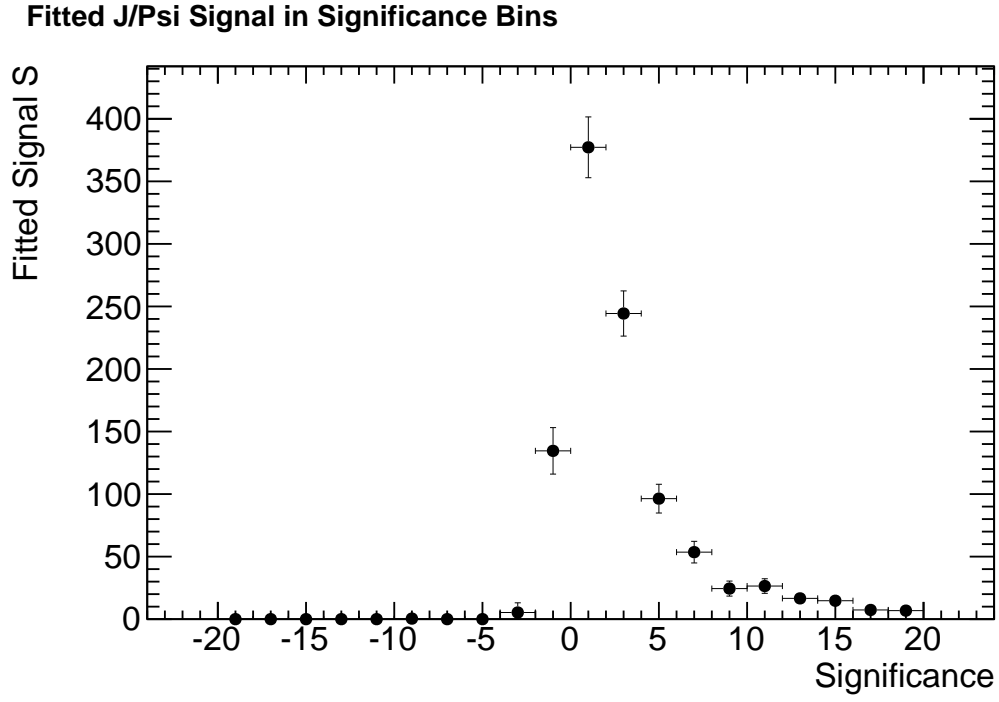


Figure 10: Fitted number of J/Ψ candidates versus secondary vertex significance for the inclusive B Monte Carlo.

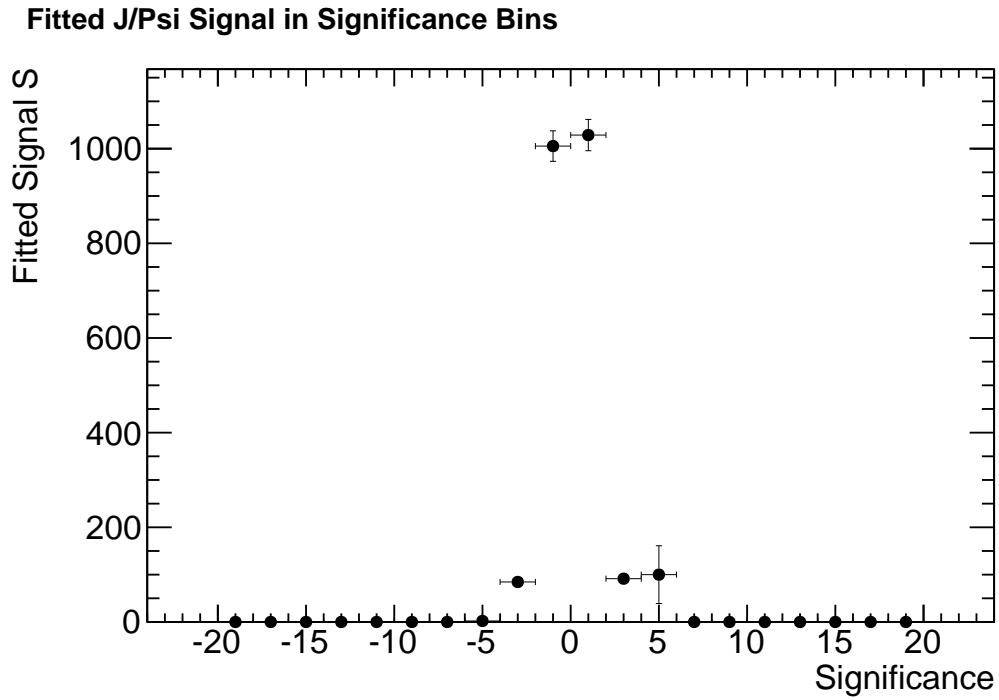


Figure 11: Fitted number of J/Ψ candidates versus secondary vertex significance for the diffractive J/Ψ Monte Carlo.

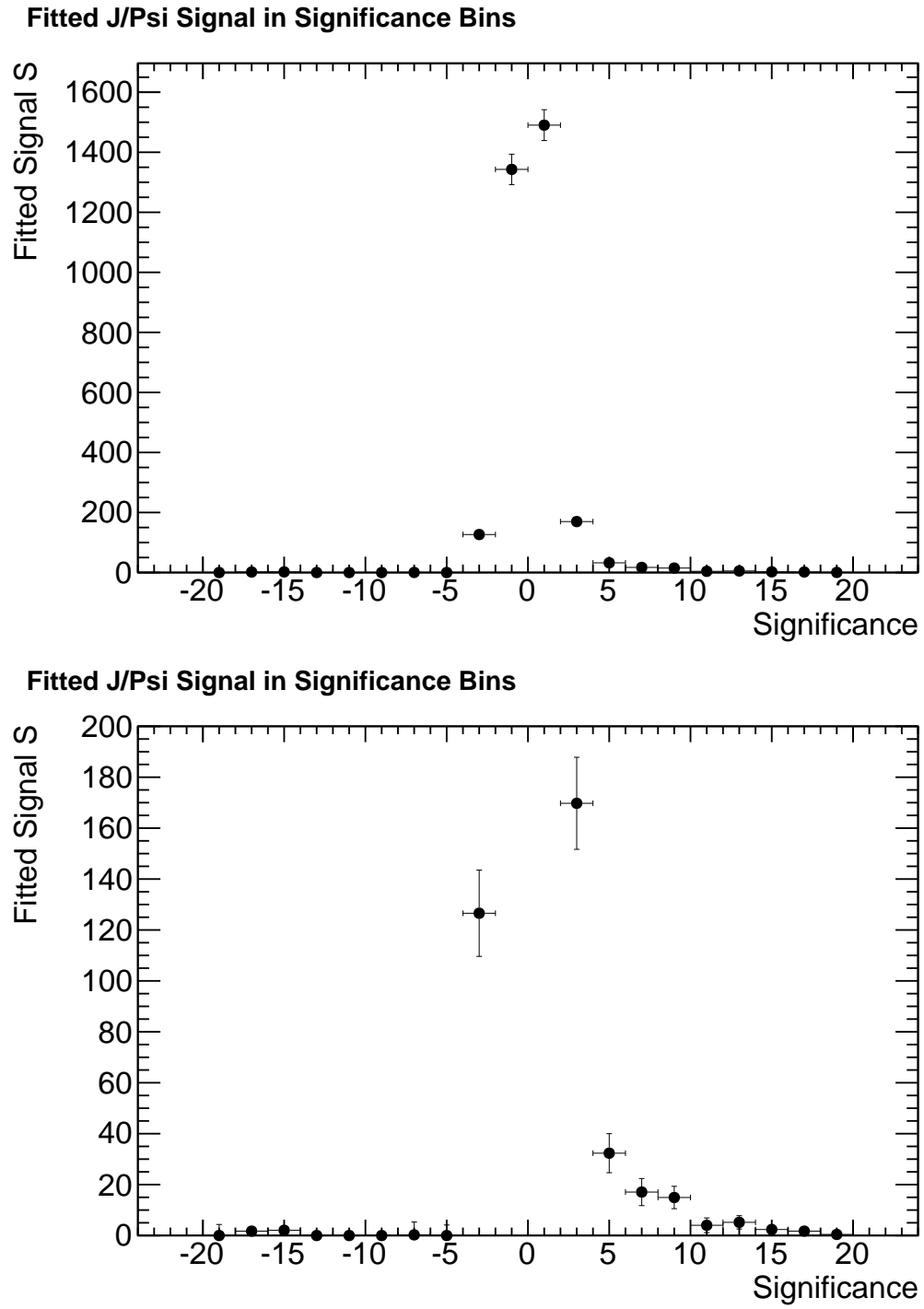


Figure 12: Fitted number of J/ψ candidates versus secondary vertex significance for the data samples. The lower graph gives a zoomed view of the upper one.

3 $B^\pm \rightarrow J/\Psi K^\pm$ Study

In the second study presented in this report I tried to do a full reconstruction of the B meson in the decay channel $B \rightarrow J/\Psi K^\pm$.

Therefore in every event with a J/Ψ -candidate this candidate is combined with every track (except the muon tracks), that fulfils the previously mentioned criteria for muon tracks. The track is given the K^\pm mass and from this the four-momentum of the assumed B -meson is calculated. The two tracks of the muons and the kaon track are used to a secondary vertex fit.

3.1 Additional Cuts

The muons used for this study have to fulfil the same criteria as in the inclusive study presented before. Furthermore the cuts on event variables are the same. Considering the cuts on the J/Ψ dependent variables it has to be stated that there is no longer a cut on the χ^2 of the fit of the two muon tracks. Instead of this a cut on the reconstructed J/Ψ -mass is introduced:

- $2.95 < m(J/\Psi) < 3.25$ GeV .

There are some additional cuts on the Kaon and the B candidate introduced:

- $P_T(K) > 200$ MeV
- $|\eta(K)| < 1.5$
- $|\eta(B)| < 1.5$
- $\chi^2/Ndf < 3$
- Vertex Significance > 3

3.2 Reconstructed B Mass

The goal of this second study is to make a B mass peak visible. Figure 14 shows the reconstructed B mass in the data sample after the final selection except cuts on χ^2/NdF and vertex significance. 13 shows the same plot for the B Monte Carlo. The red fraction of the histogram shows the contribution of those events which really contain the signal decay channel. Figures 16 and 15 show the distributions after the $\chi^2/Ndf < 3$ cut, figures 18 and 17 show the final distributions after all cuts applied.

While there is a peak at $m(B) \approx 5.28$ GeV visible that could also be fitted in all distributions for the Monte Carlo, there is no such peak in the data. Taking again in account the previously mentioned factor three to four between Monte Carlo and data this could still be in agreement.

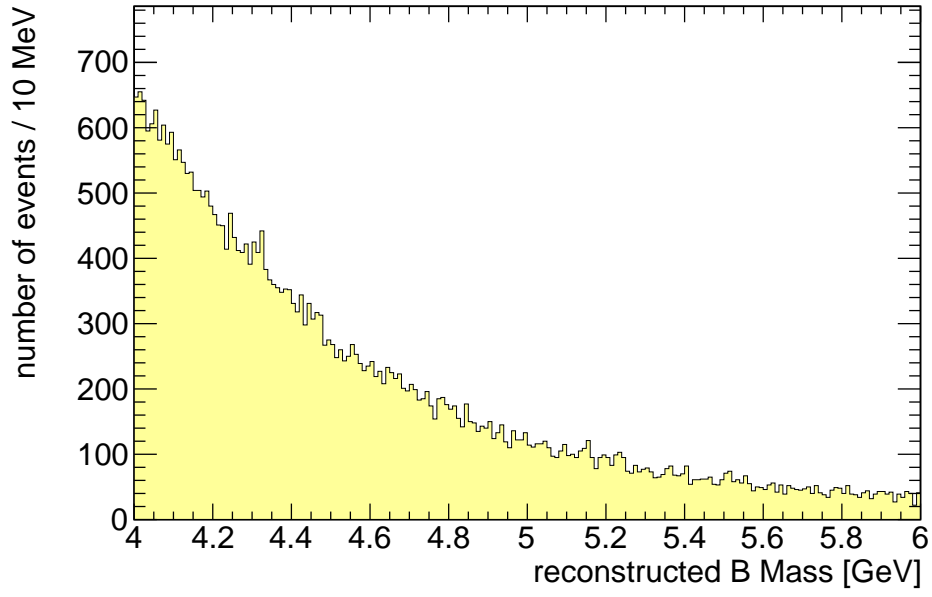


Figure 13: Distribution of reconstructed B mass in data sample after rudimentary selection.

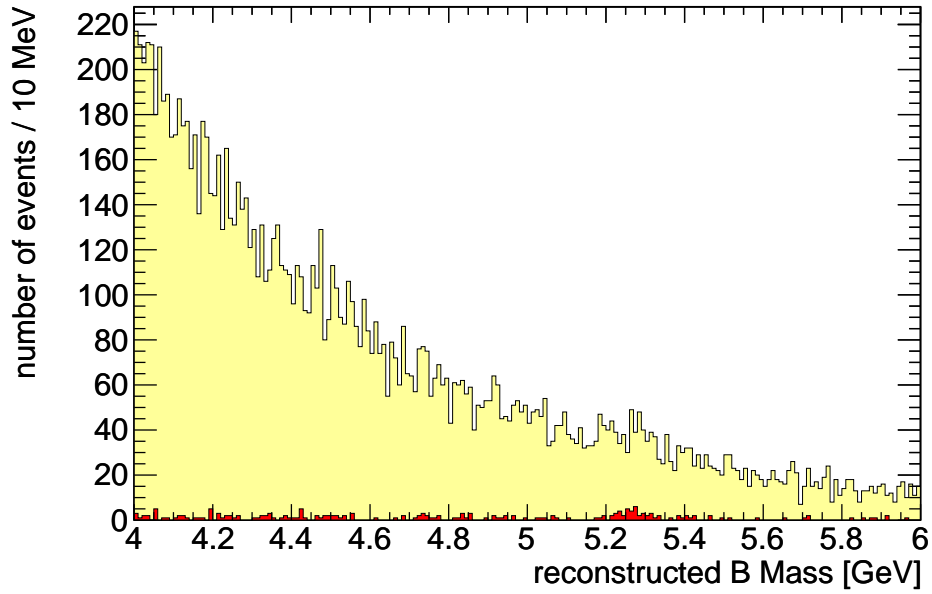


Figure 14: Distribution of reconstructed B mass in B Monte Carlo sample after rudimentary selection. The red bars indicate the contribution of events that actually contain the desired decay channel.

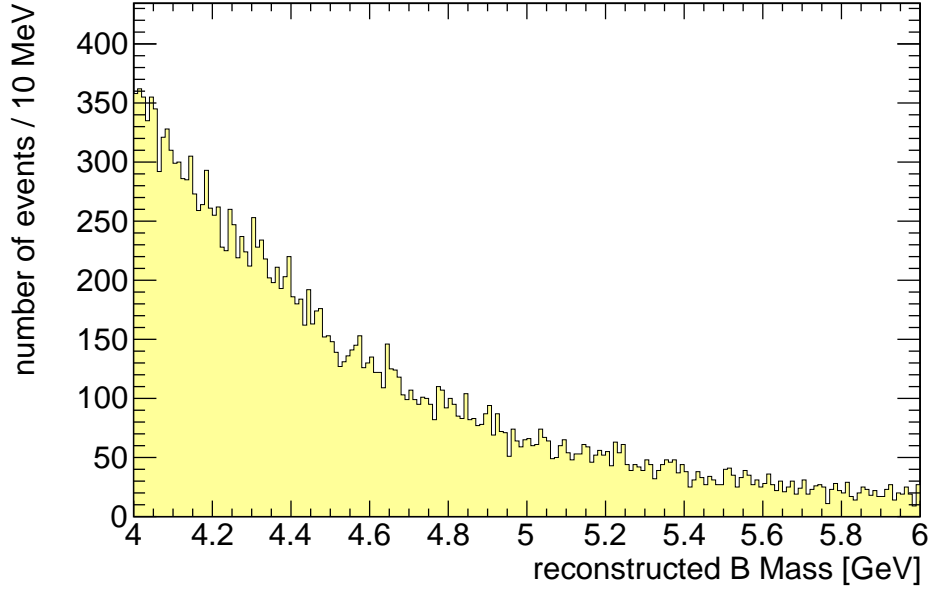


Figure 15: Distribution of reconstructed B mass in data sample after $\chi^2/Ndf < 3$ cut.

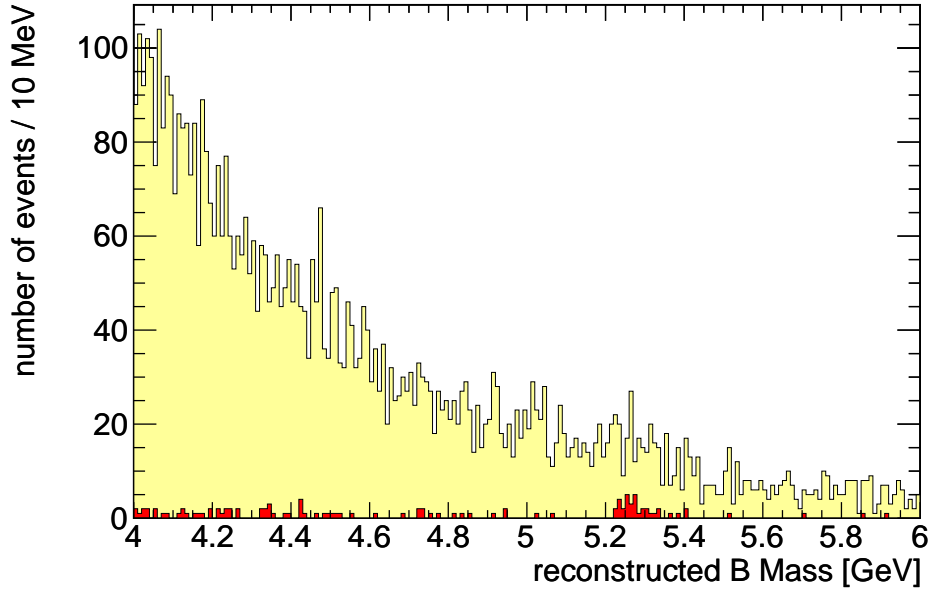


Figure 16: Distribution of reconstructed B mass in B Monte Carlo sample after $\chi^2/Ndf < 3$ cut. The red bars indicate the contribution of events that actually contain the desired decay channel.

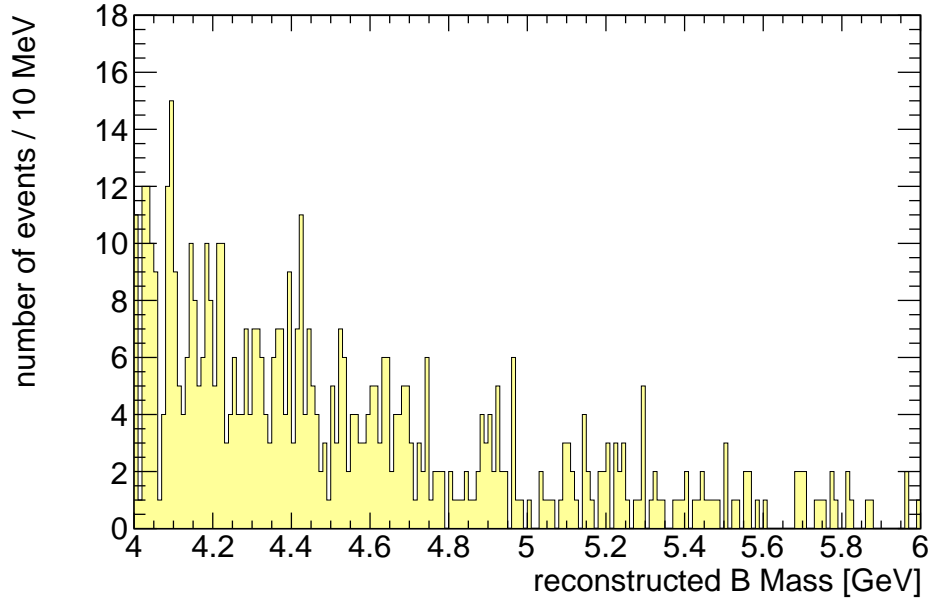


Figure 17: Distribution of reconstructed B mass in data sample after vertex significance > 3 cut.

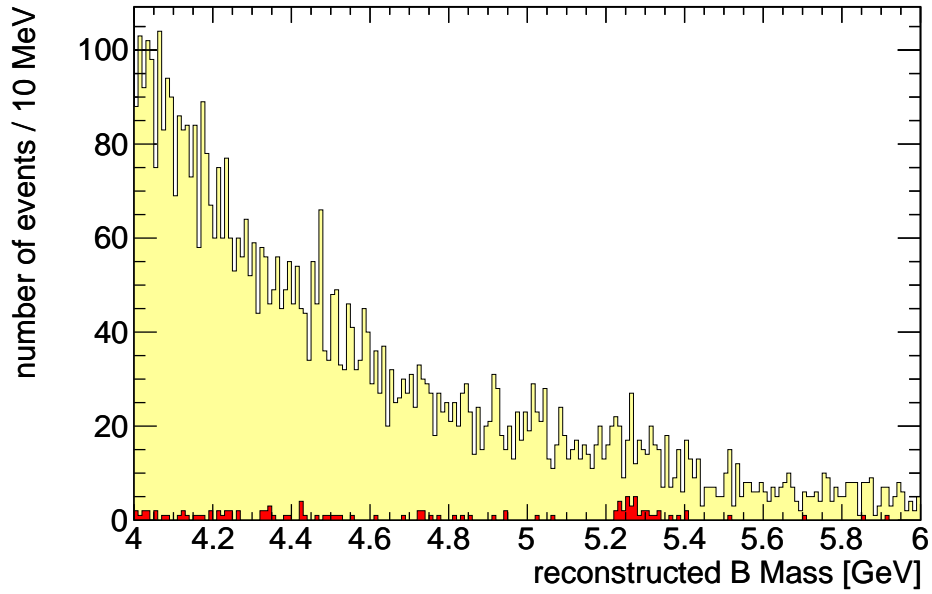


Figure 18: Distribution of reconstructed B mass in B Monte Carlo sample after Vertex Significance > 3 cut. The red bars indicate the contribution of events that actually contain the desired decay channel.

4 Conclusion

In my studies I could establish the $B \rightarrow J/\Psi X$ decay via an inclusive J/Ψ secondary vertexing method. I found a J/Ψ signal originating from secondary vertices at an confidence level of approximately 5σ . This significance could in future studies even be enhanced if the shape of the signal distribution over the secondary vertex significance is used. In my studies I only distinguished between positive and negative significance to determine the asymmetry.

The complete B reconstruction in the decay $B^\pm \rightarrow J/\Psi K^\pm$ was only successful in the dedicated B Monte Carlo. In this sample a peak is visible that can also be fitted. This peak could not be established in the data sample. A better understanding of the background and additional methods to identify the Kaon track could possibly change this. Nevertheless the very low total branching ratio of the chosen decay channel will probably always result in low statistics.

5 Acknowledgements

I would like to thank my supervisor Olaf Behnke for the many hours of lively and interesting explanations and his helpful hints and proposals for the project. Furthermore I would like to thank the DESY for giving me the opportunity to take part in the summer student program.

References

- [1] S. Lüders, *A Measurement of the Beauty Production Cross Section via $B \rightarrow J/\Psi X$ at HERA*, Ph.D. thesis, Swiss Feder Institute of Technology Zurich, (Nov. 2001).
- [2] *tLite Web Site*,
https://www-zeus-data.desy.de/tracking/ZEUS_ONLY/tools/tLite/.